nature nanotechnology

LETTERS

PUBLISHED ONLINE: 28 NOVEMBER 2010 | DOI: 10.1038/NNANO.2010.232

Highly conductive, printable and stretchable composite films of carbon nanotubes and silver

Kyoung-Yong Chun[1†], Youngseok Oh[2†], Jonghyun Rho[3], Jong-Hyun Ahn[2,3], Young-Jin Kim[1,2], Hyouk Ryeol Choi[1] and Seunghyun Baik[1,2,4*]

Conductive films that are both stretchable and flexible could have applications in electronic devices[1,2], sensors[3,4], actuators[5] and speakers[6]. A substantial amount of research has been carried out on conductive polymer composites[7], metal electrode-integrated rubber substrates[8–10] and materials based on carbon nanotubes and graphene[1,2,11–13]. Here we present highly conductive, printable and stretchable hybrid composites composed of micrometre-sized silver flakes and multiwalled carbon nanotubes decorated with self-assembled silver nanoparticles. The nanotubes were used as one-dimensional, flexible and conductive scaffolds to construct effective electrical networks among the silver flakes. The nanocomposites, which included polyvinylidenefluoride copolymer, were created with a hot-rolling technique, and the maximum conductivities of the hybrid silver–nanotube composites were 5,710 S cm^{-1} at 0% strain and 20 S cm^{-1} at 140% strain, at which point the film ruptured. Three-dimensional percolation theory reveals that Poisson's ratio for the composite is a key parameter in determining how the conductivity changes upon stretching.

Useful combinations of conductivity and stretchability have been observed in vertically aligned multiwalled carbon nanotube (MWNT) forest/polyurethane films (~0.5–1 S cm^{-1} at 0% strain and electrical resistance increased upon stretching[12]) and in textiles coated with single-walled carbon nanotube (SWNT) inks (~125 S cm^{-1}, ref. 13), but these materials do not have the printability that is required for the complex interconnects found in mass-produced electronic systems. Printable composites with a conductivity of 57 S cm^{-1} at 38% tensile strain have been synthesized using ionic liquid, fluorinated copolymer and ultralong SWNTs, with the stretchability being further improved at the expense of maximum conductivity (which fell to 6 S cm^{-1} at 134% strain) by perforating the nanotube film and then coating it with polydimethylsiloxane (PDMS)[1]. Jet milling has also been used to improve the performance of nanotube films (without perforation) to a maximum conductivity of 102 S cm^{-1} at 29% strain (15.8 wt% of SWNTs) or 9.7 S cm^{-1} at 118% strain (1.4 wt% of SWNTs)[11]. However, the conductivity of stretchable and printable composites needs to improve further if it is to compete with the high conductivity of metals.

Figure 1 shows a schematic of the preparation of a hybrid Ag–MWNT composite film (detailed procedures are described in Methods). In brief, silver nanoparticles with phenyl rings were synthesized using the self-assembly method[14–17] (Fig. 1a) and conjugated with nanotubes by means of a π–π interaction to produce nAg–MWNTs (Fig. 1b). The conjugation of MWNTs and silver nanoparticles with an average size of 3 nm was confirmed by high-resolution transmission electron microscopy (HRTEM), X-ray photoelectron spectroscopy (XPS) and energy dispersive X-ray analysis (EDS, see Supplementary Fig. S1). Supplementary Fig. S2 compares bucky films formed from bare MWNTs and from nAg–MWNTs (see Supplementary Information). A uniform film could be achieved using nAg–MWNTs, whereas cracks were observed when using bare MWNTs, possibly due to the increased surface roughness of nAg–MWNTs contributing to friction against slip during the drying process. The nanotubes decorated with silver nanoparticles led to the construction of an effective mechanical network. The nAg–MWNTs were mixed with 1-butyl-4-methylpyridinium tetrafluoroborate to make a gel (Fig. 1c). Ionic liquids are used to make conductive nanotube gels because of their high ionic conductivity, thermal stability and dispersability[1,11,18–20]. The pyridinium-based ionic liquid was selected for this study because of the resultant low surface damage of the nanotubes after mixing[21]. The nAg–MWNT gel and silver flakes were mixed and sonicated in a polyvinylidenefluoride (PVDF) solution (Figs. 1d,e). A flake form of silver was used because of its larger contact area compared with the spherical form, and PVDF copolymer was chosen as the matrix because of its good electrical and mechanical properties. The optimized ionic liquid concentration in the PVDF matrix was found to be 2.4 wt%, which provided the lowest resistance (Supplementary Fig. S3). Electron flow occurred by self-ion diffusion in the film[22]. Finally, the hybrid Ag–MWNT composite film with an average thickness of 140 μm was prepared by drop casting, drying and curing at 160 °C.

The conductivity of the hybrid Ag–MWNT film was investigated as a function of curing temperature (Supplementary Fig. S4). The conductivity increased with an increase in curing temperature due to shrinkage of the polymer matrix[17,23]. It is well known that the coalescence of silver nanoparticles can be achieved at temperatures significantly lower than the melting temperature of bulk silver because of the large surface area and instability of the surface atoms[17]. Indeed, sintering of silver nanoparticles attached on the surfaces of nanotubes was observed at 178 °C (ref. 17). This leads to an increase in conductivity, but a decrease in stretchability, which precisely matches the experimental observations in this study (Supplementary Fig. S4). The curing temperature was therefore set at 160 °C to induce polymer shrinkage but prevent sintering of the silver nanoparticles.

The hybrid Ag–MWNT film was easily peeled off a glass petri dish after the curing procedure (Fig. 2a). The film was homogeneous, as shown in the inset of Fig. 2a, and silver flakes and nAg–MWNTs embedded in the polymer matrix could be observed in a magnified scanning electron microscope (SEM) image (Fig. 2b).

[1]School of Mechanical Engineering, Sungkyunkwan University, Suwon, 440-746, Korea, [2]SKKU Advanced Institute of Nanotechnology (SAINT), Sungkyunkwan University, Suwon, 440-746, Korea, [3]School of Advanced Materials Science & Engineering, Sungkyunkwan University, Suwon, 440-746, Korea, [4]Department of Energy Science, Sungkyunkwan University, Suwon, 440-746, Korea; †These authors contributed equally to this work.
*e-mail: sbaik@me.skku.ac.kr

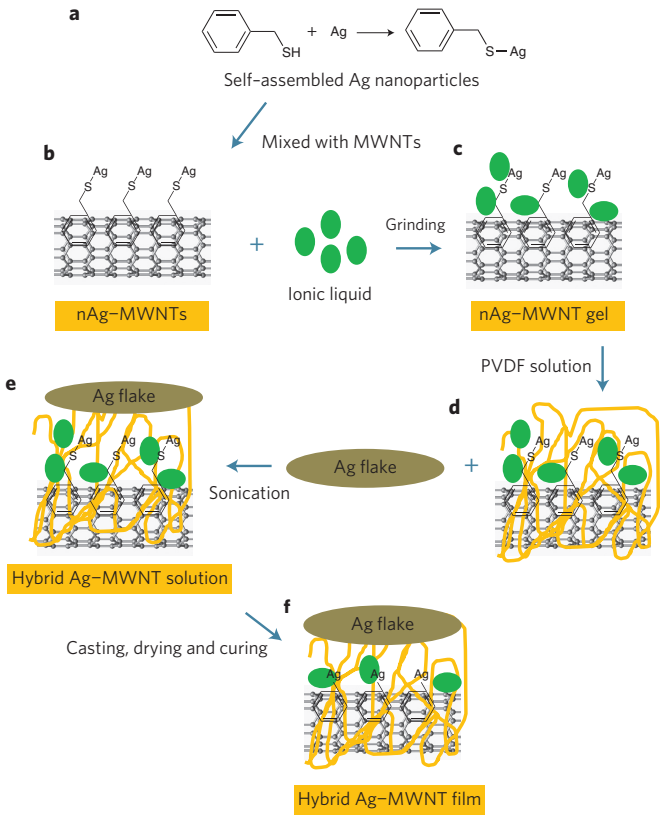

Figure 1 | Schematic of the preparation of a hybrid Ag–MWNT composite film. a, Silver nanoparticles with phenyl rings were synthesized by means of the self-assembly method. **b**, Multiwalled carbon nanotubes decorated with silver nanoparticles (nAg–MWNTs). **c**, nAg–MWNT gel was prepared by mixing and grinding nAg–MWNTs with ionic liquid (1-butyl-4-methylpyridinium tetrafluoroborate). **d**, nAg–MWNT gel was blended and sonicated in PVDF solution (560 W for 5 min). **e**, Hybrid Ag–MWNT solution was prepared by sonicating silver flakes in nAg–MWNT/PVDF solution (560 W for 10 min). The average size of the silver flakes was 3 μm. **f**, Hybrid Ag–MWNT composite film was finally obtained by drop casting, drying and curing.

Figure 2c shows the conductivity of the hybrid Ag–MWNT film at 0% strain as a function of the mass fraction of silver flakes. The mass of the other components was fixed (nAg–MWNTs, 100 mg; ionic liquid, 200 mg; PVDF solution, 8.2 g). The relative concentration of the self-assembled silver nanoparticles and nanotube scaffolds was optimized at nAg:MWNTs = 30:70 wt% (Supplementary Fig. S5). The conductivity of the hybrid Ag–MWNT film rapidly increased when silver flakes were added at a level greater than 6.07 wt% (experimentally observed percolation threshold) and reached a maximum value of 3.1×10^3 S cm^{-1} at 8.60 wt%. The addition of silver flakes above 8.60 wt% resulted in a brittle film with phase separation. A pure silver flake film (Ag:ionic liquid + PVDF solution = 10:90 wt%) was non-stretchable and had a relatively low conductivity of 525 S cm^{-1}. The theoretical prediction for the conductivity of the composite was obtained using a power-law relationship and three-dimensional percolation theory (see Supplementary Information). Briefly, the power-law relationship[24] is described by

$$\sigma = \sigma_0(V_f - V_c)^s \quad (1)$$

where σ is the electrical conductivity of the composite, σ_0 is the conductivity of the conductive filler, V_f is the volumetric fraction of the filler, V_c is the volumetric fraction at the percolation threshold, and s is the fitting exponent. Silver flakes were modelled as uniformly distributed nanoplatelets with a random orientation, and the percolation threshold was calculated using the average interparticle distance model[24]. The calculated percolation threshold (16.13 vol% after the drying process, which is equivalent to 6.07 wt% in the initial mixture) and power-law fitting provided good agreement with the experimental data until phase separation of silver flakes was observed at 9.09 wt%. As shown in Fig. 2d, the conductivity of the hybrid Ag–MWNT film (20 × 5 × 0.14 mm) was measured under varying tensile strains using a four-point probe system. The conductivity measurement system is described in the Supplementary Information (Fig. S6). The conductivity of the hybrid Ag–MWNT film decreased with increasing strain, and a conductivity of 706S cm^{-1} was obtained at 30% strain (silver flake concentration, 8.60 wt%). The amount of silver flakes (~6.07–8.60 wt%) rarely affected stretchability, and all films ruptured at ~35% tensile strain. Repeatability test results up to 5,000 cycles are shown in the inset of Fig. 2d. Conductivity initially decreased, then reached a stable value of 1,510 S cm^{-1}.

The electrical performance of the hybrid Ag–MWNT film was visually demonstrated using light-emitting diode (LED) chips, as schematically illustrated in Fig. 2e. The current–voltage response of the LEDs is shown in Fig. 2f. The LED was turned on when the applied bias was greater than 2.3 V due to the energy bandgap of the LED. The current decreased when the film was stretched using different values of tensile strain (up to 30%). However, the current–voltage characteristics completely recovered when the strain was released. As a control, the LED chips were attached to a gold film by silver paste. The current–voltage response of the Ag–MWNT film was even better than the gold film at 0% strain. The contact resistance could have been generated between the LED chip and gold film due to incomplete coverage of silver paste. A visual image of the LED chips before and after stretching (30% strain) is shown in Fig. 2g.

The stretchability of the Ag–MWNT film was improved by optimization of the geometry, as shown in Fig. 3a. Stretchability improved from 30 to 35% by introducing two circular holes, each with a diameter of 1 mm, into the Ag–MWNT film. Such perforation can induce discontinuities in the stress distribution and increase elasticity under tensile load[25]. Although circular holes were used in this study, the maximum stress can be further reduced by optimizing the hole shape (Supplementary Figs S7 and S8). Stretchability was also improved by up to 75% when the Ag–MWNT film was embedded in a nitrile butadiene rubber (NBR) substrate (without perforation[26]). This confirms that an elastic polymer substrate can increase the stretchability of a conductive film that is embedded in the substrate, while maintaining its high conductivity[1,3,7–10,27]. Stretchability was further improved to 120% when the Ag–MWNT film embedded in the NBR substrate was perforated with circular holes. A conductivity of 300 S cm^{-1} was achieved at a strain of 120% (8.6 wt% silver flakes), which is the highest conductivity obtained to date, under equivalent strain, when compared with other types of perforated or polymer-embedded conductive films[1,11–13]. Fracture was initiated at the plane interface between the Ag–MWNT film and NBR substrate when further strain was applied.

Figure 3b presents a schematic of the hot-rolling process for the hybrid Ag–MWNT film. The film was hot-rolled using rotary drums, without perforation or embedding in NBR (detailed procedures are provided in the Supplementary Information, Fig. S9). This hot-rolling technology can disperse fillers effectively and densify the film, leading to a physically compact morphology[28–30]. The thickness of the film was reduced by ~5% after the hot-rolling process. Silver flakes were more uniformly distributed and compactly embedded in the polymer matrix, as confirmed by SEM images (Supplementary Fig. S10). Figure 3c presents four

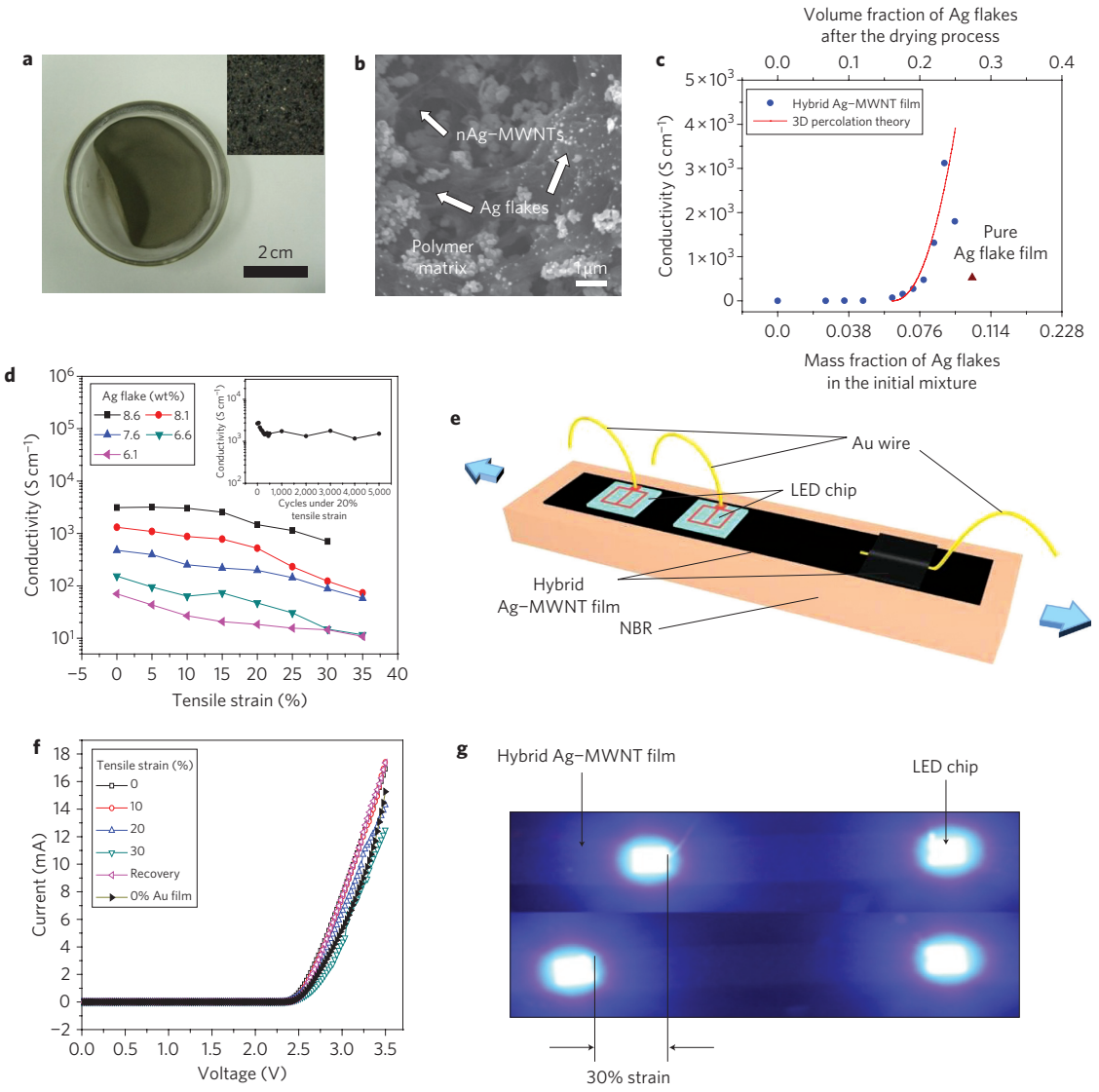

Figure 2 | Hybrid Ag–MWNT composite films. a, The cast Ag–MWNT film. Inset: magnified optical image (original magnification, ×100). **b**, SEM image. **c**, Conductivity of the hybrid Ag–MWNT film, composed of MWNTs decorated with silver nanoparticles and varying concentrations of silver flakes, investigated at 0% strain. The relative weight ratio of the self-assembled silver nanoparticles and MWNTs was fixed at 30:70 wt% (nAg:MWNTs). The conductivity of a pure silver flake film without MWNTs is also shown (purple triangle). The red line is a prediction based on a power-law relationship (equation (1) in main text) and three-dimensional percolation theory. **d**, Conductivity of the hybrid Ag–MWNT film under tensile strain for five different fractions of silver flakes. Inset: cycling tests under 20% tensile strain. **e**, Operation of LED chips connected to the hybrid Ag–MWNT film (8.6 wt% silver flakes). The film was attached on the NBR substrate. The bottom electrodes of the LEDs were attached to the Ag–MWNT film by thermal annealing (150 °C for 1 h). The top electrodes of the LEDs were connected to gold wires. A gold wire, attached to the Ag–MWNT film by thermal annealing, was used as ground. **f**, Current–voltage characteristics of LED chips measured before and after stretching for different values of tensile strain (up to 30%). The current–voltage characteristics completely recovered when the strain was released in the first cycle (recovery). As a control, LED chips were attached to a gold film with silver paste and the current measured at 0% strain. **g**, Visual images of LEDs at an applied bias of 3.3 V before (top) and after (bottom) stretching. The LED current decreased to 71.7% at 30% strain and returned to the original value after release.

sets of conductivity data for hot-rolled Ag–MWNT films as well as data for control materials[1,11–13]. The conductivities of the hot-rolled Ag–MWNT films are shown as filled symbols in the shaded region of the figure, whereas open symbols represent control materials. The initial conductivity and stretchability were increased by as much as 190 and 342%, respectively, following the hot-rolling process, although there was some variation among the different specimens. Stretching of the hot-rolled film is also shown in Supplementary Video S1. The maximum conductivities of the hot-rolled Ag–MWNT films were 5,710 S cm^{-1} at 0% strain and 20 S cm^{-1} at 140% strain. The conductivities are orders of magnitude greater than all control materials up to ~50% strain, and still higher than other printable composites up to 140% strain. The conductivity of the MWNT forest/polyurethane film was ~0.5–1 S cm^{-1} at 0% strain[12]. The sheet electrical resistance normalized by the initial resistance at zero strain, R/R_0, increased upon stretching, and was ~4.2 at 300% strain[12]. The conductivity of the textile coated with SWNT ink was ~125 S cm^{-1} (ref. 13). The value of R/R_0 decreased to ~0.825 until the strain reached 140%, and then increased as the strain increased further (~0.95 at 229% strain)[13]. The MWNT forest/polyurethane film and the textile coated with SWNT ink exhibited higher stretchability or conductivity in the high strain region. However, these materials are not compatible with the printing process required for mass-produced electronic systems.

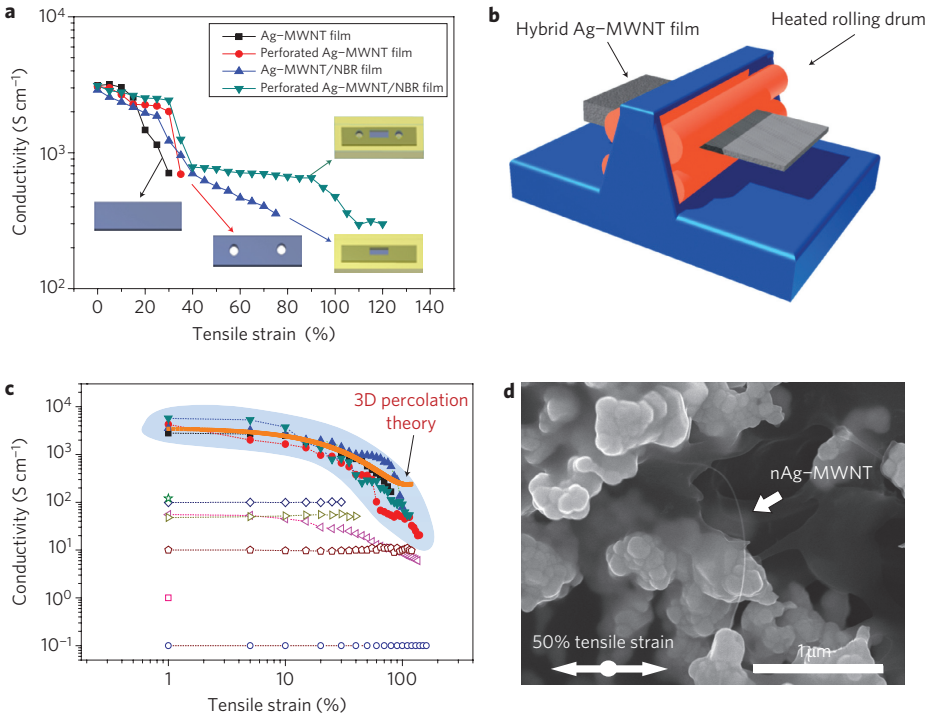

Figure 3 | Conductivity and stretchability of various hybrid Ag–MWNT films. a, Conductivity and stretchability were significantly improved when the Ag–MWNT film was perforated and embedded in NBR. **b**, Schematic of the hot-rolling process for the hybrid Ag–MWNT film. **c**, Conductivities of hot-rolled Ag–MWNT films compared with those of control materials. Filled symbols: hot-rolled Ag–MWNT films. Open symbols: triangles, diamonds, pentagons, super growth SWNT films[1,11]; magenta open square, MWNT forest/polyurethane film[12]; green open star, textile coated with SWNT ink[13]; blue open circles, commercial conducting rubber[1]. The conductivity calculated using three-dimensional percolation theory is shown as a solid orange line in the shaded region. **d**, SEM image of the hot-rolled Ag–MWNT film at 50% tensile strain.

Electrical conductivity calculated using three-dimensional percolation theory is shown as a solid orange line in the shaded region of Fig. 3c. Poisson's ratio emerged as a key parameter, and a detailed derivation is provided in the Supplementary Information. The total volume of the composite changed on stretching, which could be calculated as a function of the strain and Poisson's ratio, but other parameters in the power-law relationship were assumed to be constant. The hot-rolled Ag–MWNT film was non-isotropic, and two experimentally measured values of Poisson's ratio in the direction of the thickness and width ($\nu_t = 0.24$, $\nu_w = 0.13$) were used in the calculation. The theoretical prediction could describe the experimental data well, although it overestimated the data in the region of high strain. The theory assumes uniform filler distribution upon stretching of the film. However, this assumption fails at high strain, where experimentally measured conductivity decreases rapidly, leading to overestimation of the theory. Figure 3d shows an SEM image of the hot-rolled Ag–MWNT film at 50% strain. The nAg–MWNT, forming an electrical network between the silver flakes, is clearly shown. The silver nanoparticles on MWNTs therefore improved the contact interface with the silver flakes[17].

The significant decrease in conductivity of the composite film with increasing tensile strain may cause problems, particularly in practical applications in the region of high strain. According to the power-law relationship of equation (1), this can be minimized or overcome by using a matrix polymer with a high Poisson's ratio, because the decrease in V_f or increase in total volume can be reduced. A composite with an excessive amount of silver may exhibit long-term instability, because phase separation of silver was observed when the concentration was higher than 8.6 wt%. Better dispersion techniques with ultrasonication, shear mixing and hot-rolling processes would enable a more uniform filler distribution at high silver concentrations, which should lead to improved long-term reliability.

Methods

Synthesis of the Ag–MWNT film. Silver nanoparticles were synthesized by stirring 400 ml $AgNO_3$ solution in ethanol (Junsei, 0.02 mol l^{-1}) with 100 ml benzyl mercaptan solution in ethanol (Sigma Aldrich, 0.06 mol l^{-1}) for 48 h (refs 15–17). Thin MWNTs with an outer diameter of 4 nm (Hanwha Nanotech, 50 mg), dispersed by sonication (SMT Co., UH-50, 560 W, 10 min) in ethanol (1.8 wt%), were mixed with the 500 ml of silver nanoparticle solution by sonication in a bath (200 W, 6 h). The nanotubes decorated with silver nanoparticles (nAg–MWNTs) were obtained by filtering several times (PTFE membrane, 0.2 μm) and ethanol rinsing. Silver nanoparticles were adsorbed on nanotubes by means of a π–π interaction[17].

In the next step, 100 mg nAg–MWNTs were ground with 200 mg ionic liquid (1-butyl-4-methylpyridinium tetrafluoroborate) using a pestle and mortar for 30 min to yield a black gel[1,11]. The nAg–MWNT gel (300 mg) was mixed with a fluorinated copolymer, 10 mg of PVDF copolymer in 4-methyl-2-pentanone (2.6 wt%), and sonicated at room temperature (560 W, 5 min). Silver flakes (Ferro, silver flake #120) with an average size of 3 μm were added into the solution and sonicated (560 W, 10 min). Finally, the hybrid Ag–MWNT film was obtained by drop casting, drying (12 h) and curing (160 °C) on a petri dish. The final dimensions of the film were 20 × 5 × 0.14 mm. The hybrid Ag–MWNT film was also passed through hot-rolling equipment (Grand Digital Plus 350, 140 °C) with a roller gap size of 0.1 mm. Stretchability could be increased by embedding in NBR or perforation. The hybrid Ag–MWNT film was embedded into the NBR by means of a two-stage curing process (60 °C for 6 h, 155 °C for 15 min)[26]. Two circular holes with a diameter of 1 mm were introduced into the film by perforation.

Characterization. The adsorption of silver nanoparticles on thin MWNTs was investigated by field-emission SEM (JEOL, JSM 890), HRTEM (JEOL, 300 kV), XPS (VG–Scientific Escalab 250, Al-Ka line, 1,486.6 eV with 0.1 eV resolution) and EDS (JSM 890). The conductivity of the film was measured using a four-point probe in-line method[16,17,23]. A nanovoltmeter (Keithley 2182A) was used at a constant current of 20 μA (Keithley 6221). Tensile strain was applied using a house-built device. Operation of the hybrid Ag–MWNT film was demonstrated using LED chips (CREE, C460EZ700-S24000). Top electrodes of LED chips were connected to gold wires using a wire bonder (WEST BOND, Model 7600D). The operation of the LED chips was also confirmed using a current meter (Keithley 6485) up to 30% tensile strain.

Received 9 July 2010; accepted 25 October 2010; published online 28 November 2010

References

1. Sekitani, T. *et al.* A rubberlike stretchable active matrix using elastic conductors. *Science* **321,** 1468–1472 (2008).
2. Kim, K. S. *et al.* Large-scale pattern growth of graphene films for stretchable transparent electrodes. *Nature* **457,** 706–710 (2009).
3. Someya, T. *et al.* A large-area, flexible pressure sensor matrix with organic field-effect transistors for artificial skin applications. *Proc. Natl Acad. Sci. USA* **101,** 9966–9970 (2004).
4. Lee, B. Y. *et al.* Scalable assembly method of vertically-suspended and stretched carbon nanotube network devices for nanoscale electro-mechanical sensing components. *Nano Lett.* **8,** 4483–4487 (2008).
5. Sekitani, T. *et al.* A large-area wireless power-transmission sheet using printed organic transistors and plastic MEMS switches. *Nature Mater.* **6,** 413–417 (2007).
6. Xiao, L. *et al.* Flexible, stretchable, transparent carbon nanotube thin film loudspeakers. *Nano Lett.* **8,** 4539–4545 (2008).
7. Hansen, T. S., West, K., Hassager, O. & Larsen, N. B. Highly stretchable and conductive polymer material made from poly(3,4-ethylenedioxythiophene) and polyurethane elastomers. *Adv. Funct. Mater.* **17,** 3069–3073 (2007).
8. Khang, D. Y., Jiang, H. Q., Huang, Y. & Rogers, J. A. A stretchable form of single-crystal silicon for high-performance electronics on rubber substrates. *Science* **311,** 208–212 (2006).
9. Sun, Y. G. *et al.* Controlled buckling of semiconductor nanoribbons for stretchable electronics. *Nature Nanotech.* **1,** 201–207 (2006).
10. Kim, D. H. *et al.* Stretchable and foldable silicon integrated circuits. *Science* **320,** 507–511 (2008).
11. Sekitani, T. *et al.* Stretchable active-matrix organic light-emitting diode display using printable elastic conductors. *Nature Mater.* **8,** 494–499 (2009).
12. Shin, M. K. *et al.* Elastomeric conductive composites based on carbon nanotube forests. *Adv. Mater.* **22,** 2663–2667 (2010).
13. Hu, L. *et al.* Stretchable, porous, and conductive energy textiles. *Nano Lett.* **10,** 708–714 (2010).
14. Yang, D-Q., Hennequin, B. & Sacher, E. XPS demonstration of π–π interaction between benzyl mercaptan and multiwalled carbon nanotubes and their use in the adhesion of Pt nanoparticles. *Chem. Mater.* **18,** 5033–5038 (2006).
15. Yang, G-W. *et al.* Controllable deposition of Ag nanoparticles on carbon nanotubes as a catalyst for hydrazine oxidation. *Carbon* **46,** 747–752 (2008).
16. Oh, Y., Suh, D., Kim, Y-J., Han, C.-S. & Baik, S. Transparent conductive film fabrication using intercalating silver nanoparticles within carbon nanotube layers. *J. Nanosci. Nanotech.* (in the press).
17. Oh, Y., Chun, K-Y., Lee, E., Kim, Y.-J. & Baik, S. Nano-silver particles assembled on one-dimensional nanotube scaffolds for highly conductive printable silver/epoxy composites. *J. Mater. Chem.* **20,** 3579–3582 (2010).
18. Mukai, K. *et al.* High performance fully plastic actuator based on ionic-liquid-based bucky gel. *Electrochim. Acta* **53,** 5555–5562 (2008).
19. Kim, D-W., Sivakkumar, S. R., MacFalane, D. R., Forsyth, M. & Sun, Y-K. Cycling performance of lithium metal polymer cells assembled with ionic liquid and poly(3-methyl thiophene)/carbon nanotube composite cathode. *J. Power Sources* **180,** 591–596 (2008).
20. Price, B. K., Hudson, J. L. & Tour, J. M. Green chemical functionalization of single-walled carbon nanotubes in ionic liquids. *J. Am. Chem. Soc.* **127,** 14867–14870 (2005).
21. Jarosik, A., Krajewski, S. R., Lewandowski, A. & Radzimski, P. Conductivity of ionic liquids in mixtures. *J. Mol. Liq.* **123,** 43–50 (2006).
22. Hayamizu, K., Aihara, Y., Nakagawa, H., Nukuda, T. & Price, W. S. Ionic conduction and ion diffusion in binary room-temperature ionic liquids composed of [emim][BF_4] and $LiBF_4$. *J. Phys. Chem. B.* **108,** 19527–19532 (2004).
23. Oh, Y. *et al.* Silver-plated carbon nanotubes for silver/conducting polymer composites. *Nanotechnology* **19,** 495602 (2008).
24. Li, J. & Kim, J. Percolation threshold of conducting polymer composites containing 3D randomly distributed graphite nanoplatelets. *Comp. Sci. Tech.* **67,** 2114–2120 (2007).
25. Shigley, J. E. & Mischeke, C. R. *Mechanical Engineering Design* 130–131 (McGraw-Hill, 2001).
26. Nguyen, H. C. *et al.* The effects of additives on the actuating performances of a dielectric elastomer actuator. *Smart Mater. Struct.* **18,** 015006 (2009).
27. Lacour, S. P., Jones, J. E., Wagner, S., Li, T. & Suo, Z. Stretchable interconnects for elastic electronic surfaces. *Proc. IEEE* **93,** 1459–1467 (2005).
28. Pavlygo, T. M., Serdyuk, G. G., Svistun, L. I., Plomod'yalo, R. L. & Plomod'yalo, L. G. Hot pressing technology to produce wear-resistant P/M structural materials with dispersed solid inclusions. *Powder Metall. Met. Ceram.* **44,** 341–346 (2005).
29. Moromoto, Y., Hayashi, T. & Takei, T. Mechanical behavior of powders during compaction in a mold with variable cross sections. *Int. J. Powder Metall. Powder Tech.* **18,** 129–145 (1982).
30. Gethin, D. T., Tran, D. V., Lewis, R. W. & Ariffin, A. K. An investigation of powder compaction processes. *Int. J. Powder Metall.* **30,** 385–398 (1994).

Acknowledgements

This work was supported by the Basic Science Research Programme (grant no. 2009-0090017) through the National Research Foundation of Korea (NRF), the Center for Nanoscale Mechatronics & Manufacturing (grant no. 2009K000160) which is a 21st-Century Frontier Research programme, and the World Class University programme (grant no. R31-2008-000-10029-0) funded by the Ministry of Education, Science and Technology, Korea.

Author contributions

K-Y.C., Y.O. and S.B. conceived and designed the experiments, which were carried out by K-Y.C., Y.O. and J.R. H.R.C. provided nitrile butadiene rubber. Y-J.K. designed the finite element modelling, and J-H.A. designed the stretching and light-emitting diode experiments. K-Y.C., Y.O. and S.B. wrote the paper. All authors contributed to data analysis and scientific discussion.

Additional information

The authors declare no competing financial interests. Supplementary information accompanies this paper at www.nature.com/naturenanotechnology. Reprints and permission information is available online at http://npg.nature.com/reprintsandpermissions/. Correspondence and requests for materials should be addressed to S.B.